

Role of the dimerized gap due to anion ordering in spin-density wave phase of $(\text{TMTSF})_2\text{ClO}_4$ at high magnetic fields

N. Matsunaga*

*Division of Physics, Hokkaido University, Sapporo 060-0810, Japan;
CRTBT-CNRS, Laboratoire Associé à l'UJF, BP 166, 38042 Grenoble, Cedex 9, France;
Grenoble High Field Laboratory, CNRS/MPI-FKF, BP 166, 38042 Grenoble, Cedex 9, France*

A. Ayari and P. Monceau

*CRTBT-CNRS, Laboratoire Associé à l'UJF, BP 166, 38042 Grenoble, Cedex 9, France
and Grenoble High Field Laboratory, CNRS/MPI-FKF, BP 166, 38042 Grenoble, Cedex 9, France*

A. Ishikawa and K. Nomura

Division of Physics, Hokkaido University, Sapporo 060-0810, Japan

M. Watanabe, J. Yamada, and S. Nakatsuji

Department of Material Science, Himeji Institute of Technology, Kamigohri 678-1297, Japan

(Received 25 March 2002; published 18 July 2002)

Magnetoresistance measurements have been carried out along the highly conducting a axis in the field-induced spin-density wave (FISDW) phase of hydrogenated and deuterated $(\text{TMTSF})_2\text{ClO}_4$ for various cooling rates through the anion ordering temperature. With increasing the cooling rate, (i) the high-field phase boundary β_{HI} , observed at 27 T in hydrogenated samples for slowly cooled, is shifted towards a lower field, (ii) the last semimetallic SDW phase below β_{HI} is suppressed, and (iii) the FISDW insulating phase above β_{HI} is enhanced in both salts. The cooling rate dependence of the FISDW transition and of β_{HI} in both salts can be explained by taking into account the peculiar SDW nesting vector stabilized by the dimerized gap due to anion ordering.

DOI: 10.1103/PhysRevB.66.024425

PACS number(s): 75.30.Fv, 72.15.Gd, 74.70.Kn

I. INTRODUCTION

The quasi-one-dimensional (Q1D) organic compounds $(\text{TMTSF})_2X$, where TMTSF denotes tetramethyltetraselenafulvalene and $X = \text{PF}_6$, AsF_6 , ClO_4 , etc., show many interesting phenomena such as superconductivity, anion ordering (AO), spin-density wave (SDW), a cascade of field-induced SDW (FISDW).¹ The phase diagram of the FISDW phase in the PF_6 salt, with quantized Hall resistance $\rho_{xy} \sim h/(n2e^2)$ in the sequence $n = \dots 4, 3, 2, 1, 0$ as the magnetic field is increased, is successfully explained by the mean-field theory named the “standard model” based on the nesting of a pair of slightly warped parallel sheets of the Q1D Fermi surface. The states labeled with integer n have been identified as semimetallic FISDW states while that with $n = 0$ is a FISDW insulating state. However, the phase diagram of the FISDW phase in hydrogenated $(\text{TMTSF}-h_{12})_2\text{ClO}_4$ (abbreviated as $h\text{-ClO}_4$ hereafter) for the case of slow cooling is known to show disagreements with the standard model i.e., (i) in the low-field cascade of FISDW transitions, the sequence of Hall plateaus is not in the expected order.² (ii) a very stable quantum Hall state is observed from 7.5 to 27 T.^{3,4} (iii) the FISDW transition temperature $T_{\text{FISDW}} (\sim 5.5 \text{ K})$ is independent of field above 15 T.⁵ In order to explain the differences between PF_6 and ClO_4 salts, attention has been focused on the anion ordering which occurs in $h\text{-ClO}_4$ at 24 K and dimerizes the system along the b direction by a superlattice

potential V with a wave vector $Q = (0, 1/2, 0)$.⁶ This dimerization separates the original Fermi surface (FS) into two pairs of open orbit FS sheets. Although the FISDW phase diagram in the slowly cooled $h\text{-ClO}_4$ salt is widely investigated experimentally and theoretically, however, it is still in question.

When the $h\text{-ClO}_4$ salt is rapidly cooled through the anion ordering temperature T_{AO} , the orientations of anions are frozen in two directions at random probability and the SDW phase is induced. In general, the deuteration of the TMTSF salt is thought to work as a positive chemical pressure in the crystal.⁷ When the positive chemical pressure by deuteration is applied to the ClO_4 salt, the nesting of the Q1D Fermi surface becomes more imperfect and the stabilization of the SDW phase in the intermediate cooled states is suppressed. As a result, the deuterated $(\text{TMTSF}-d_{12})_2\text{ClO}_4$ salt (abbreviated as $d\text{-ClO}_4$ hereafter) is expected to show the FISDW phase in a broad range of cooling rates in contrast with the case of hydrogenated ones.

In this paper, we describe the cooling rate \mathfrak{R}_C dependence of the FISDW phase diagram for the hydrogenated, for the smallest cooling rate accessible: 0.0009 K/s, and deuterated, for different cooling rates: 0.0009, 0.018, and 0.67 K/s, ClO_4 salts under strong magnetic fields applied parallel to the c^* axis; we discuss the role of the dimerized gap due to AO controlled by the cooling rate, and that of the chemical pressure by deuteration in the FISDW phase diagram, and we compare the results in deuterated salts with those measured in hydrogenated ones.

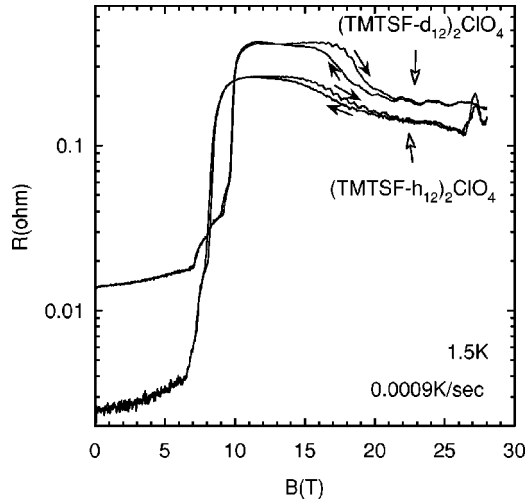


FIG. 1. Magnetoresistance along the highly conducting a axis in hydrogenated and deuterated $(\text{TMTSF})_2\text{ClO}_4$ for the relaxed state (cooling rate about 0.0009 K/s) with the magnetic field parallel to the lowest conductivity direction c^* at 1.5 K.

II. EXPERIMENT

Single crystals of $(\text{TMTSF})_2\text{ClO}_4$ were synthesized by the standard electrochemical method. The resistance measurements along the conducting a axis were carried out using a standard four-probe dc method over the temperature range from 1.5 to 10 K. The typical size of the sample was $1 \times 0.1 \times 0.1 \text{ mm}^3$. Electric leads of 10 μm gold wire were attached with silver paint onto gold evaporated contacts. The current contacts covered the whole areas of both ends of the sample for a uniform current. In order to prepare states with various degrees of anion ordering, the sample was heated up to 40 K, and then cooled again with a progressive decrease of the heating to give a controlled cooling rate \mathfrak{R}_C . The temperature was measured using a Cernox CX-1050-SD resistance thermometer calibrated by a capacitance sensor in magnetic fields. The measurements in the fields to 28 T were done in a resistive magnet at the Grenoble High Magnetic Field Laboratory.

III. RESULTS AND DISCUSSION

Figure 1 shows the magnetoresistance along the highly conducting a axis in hydrogenated and deuterated $(\text{TMTSF})_2\text{ClO}_4$ at 1.5 K for relaxed state, in which \mathfrak{R}_C is about 0.0009 K/s. Magnetic field B up to 28 T was applied parallel to the lowest conductivity direction c^* . For hydrogenated $h\text{-ClO}_4$, it is found from the sudden increase of resistance that the transitions to the first and last ($n=1$) semimetallic SDW phase take place at about 6.5 and 8 T, respectively. With increasing B , the nonoscillatory background resistance R_0 goes up and has a broad peak between 10 and 15 T and a decrease above 15 T. The magnetoresistance shows hysteresis between 14 and 21 T. The rapid oscillation (RO) is clearly seen above 14 T in Fig. 1. Above 27 T the field which was proposed by McKernan *et al.* as a new phase boundary β_{HI} of a first-order transition,⁵ both R_0 and the amplitude of RO suddenly increases; the magnetoresis-

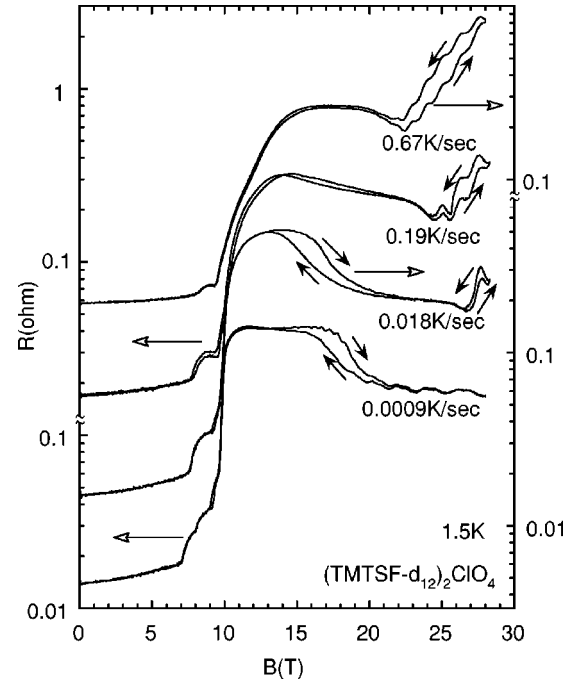


FIG. 2. Cooling rate dependence of the magnetoresistance of $(\text{TMTSF-}d_{12})_2\text{ClO}_4$ with the magnetic field parallel to the c^* direction at 1.5 K.

tance shows an isosceles triangle shape. The sudden increase of R_0 and of the RO amplitude is consistent with previous results.⁸ On the other hand, by deuteration of the ClO_4 salt, T_{AO} increases from 24 to 27 K, and the transition field to the first and last semimetallic SDW phase increases from 6.5 to 7 T and from 8 to 9.7 T, respectively. In addition, the field of the broad peak shifts to the high-field side and the phase boundary at high field β_{HI} is not observed below 28 T. This indicates that deuteration of the ClO_4 salt moves the FISDW phase boundary towards the high pressure side and β_{HI} is pushed out above 28 T. These results are regarded as the consequence of a positive chemical pressure in the crystal by deuteration.^{9,10} This is consistent with usual deuteration effects.^{7,11} Moreover, the magnetoresistance of $d\text{-ClO}_4$ shows a steplike change from the phase between 10 and 17 T to the phase above 20 T with hysteresis between 14 and 21 T. Although the possibility of a new phase boundary has been proposed around 17 T for $h\text{-ClO}_4$ from magnetoresistance measurements,¹² the origin of the above steplike magnetoresistance and hysteresis is unsolved.

The cooling rate \mathfrak{R}_C dependence of the magnetoresistance of $d\text{-ClO}_4$ at 1.5 K is shown in Fig. 2. From this figure, we find that the transition field to the last semimetallic SDW at 9.7 T is not sensitive to \mathfrak{R}_C . This means that \mathfrak{R}_C in this region does not change the effective pressure in the crystal. With increasing \mathfrak{R}_C , the sudden increase of the resistance at 9.7 T becomes rounded, and both the RO and the large hysteresis of the magnetoresistance becomes dim in the semimetallic SDW phase. Moreover, β_{HI} determined from the sudden increase of R_0 and of the RO amplitude is clearly visible and it is shifted towards a lower field with a large hysteresis in the magnetoresistance when \mathfrak{R}_C is increased. The increase

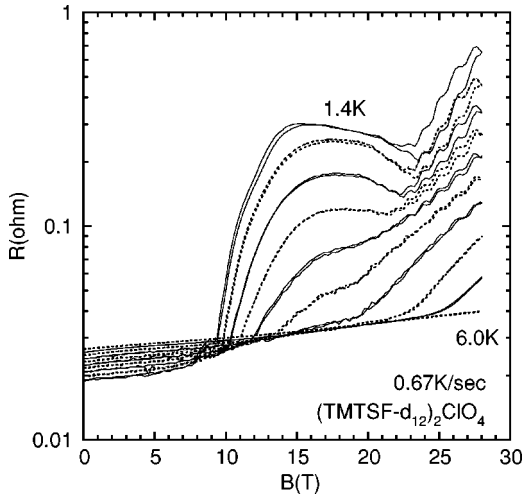


FIG. 3. Magnetoresistance of $(\text{TMTSF-}d_{12})_2\text{ClO}_4$ with the field parallel to the c^* direction for the cooling rate about 0.67 K/s at 1.3, 2.0, 2.5, 3.0, 3.5, 4.0, 4.3, 5.0, 5.5, and 6.0 K.

of the hysteresis loop above β_{HI} with increasing \mathcal{R}_C is a consequence of the broadening of the first-order transition by disorder effects. We have also measured the \mathcal{R}_C dependence of the magnetoresistance of $h\text{-ClO}_4$ and observed that β_{HI} decreases from 27 T for 0.0009 K/s to 21.5 T for 0.018 K/s, although β_{HI} becomes not very well defined for the cooling rate above 0.19 K/s. One can conclude that \mathcal{R}_C dependence of β_{HI} is a common feature in ClO_4 salts.

In Fig. 3, we show the magnetoresistance of $d\text{-ClO}_4$ at various temperatures for \mathcal{R}_C about 0.67 K/s. At this cooling rate, for each temperature, we have determined the value of the FISDW transition of $d\text{-ClO}_4$ as the intersection point between the extrapolations of the magnetoresistance curve in the FISDW and metallic phases. The FISDW transition temperature is plotted as a function of the magnetic field in Fig. 4. As shown in the upper-right side of Fig. 4, it increases with increasing the field B . This result is in agreement with previous measurements on $h\text{-ClO}_4$ for $\mathcal{R}_C=0.5$ K/s.¹³ We have previously reported the quadratic increase of T_{FISDW} with magnetic field above 12 T in $h\text{-ClO}_4$ for \mathcal{R}_C of 0.5 K/s.¹³ In the case of $d\text{-ClO}_4$, T_{FISDW} for \mathcal{R}_C of 0.67 K/s also roughly shows the quadratic field dependence above 13 T. However, for intermediate cooling rates, the quadratic field dependence of T_{FISDW} is not a quadratic increase as predicted by the mean-field theory¹⁴ but an envelope line of FISDW states with different quantum numbers n . We have also determined the value of the transition fields at β_{HI} from the intersection of the extrapolations of R_0 and have plotted them in the lower-right side of Fig. 4. As shown in Fig. 3, the large hysteresis in the magnetoresistance and RO are observed in the high-field phase region only below 3 K. Above 3 K, although the sudden increase of R_0 becomes rounded, the hump structure of R_0 exists still up to 4 K. This means that β_{HI} exists up to 4 K. The definition of our phase boundary is the same one determined by Naughton *et al.*⁴ as shown in Fig. 5. Below the magnetic field of this boundary, the nonzero Hall voltage was observed in all experiments.^{4,5}

As a result, we show in Figs. 5 and 4 the FISDW phase

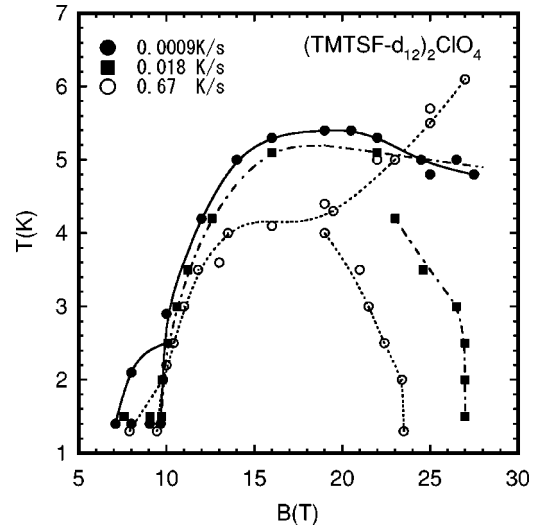


FIG. 4. The FISDW phase diagram in deuterated $(\text{TMTSF})_2\text{ClO}_4$ constructed from many temperature and field sweeps for various cooling rates. The bold, dashed-dotted, and dashed lines are guides to the eye for 0.0009, 0.018, and 0.67 K/s cooling rates, respectively.

diagram of $h\text{-ClO}_4$ and $d\text{-ClO}_4$ determined from magnetoresistance measurements for various \mathcal{R}_C , respectively. In Fig. 5, solid lines show the phase boundary for the relaxed state proposed by McKernan *et al.*⁵ The dashed line is the phase boundary of the final FISDW phase for the relaxed state originally determined by Naughton *et al.*⁴ As shown in Fig. 5, it is well known that T_{FISDW} for a slow cooling in $h\text{-ClO}_4$ is about 5.5 K and is almost independent of field B above 15

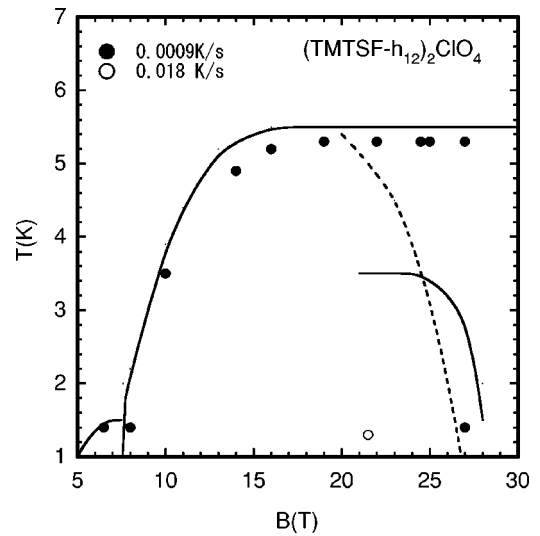


FIG. 5. The FISDW phase diagram in hydrogenated $(\text{TMTSF})_2\text{ClO}_4$ with the magnetic field parallel to the lowest conductivity direction c^* . Solid lines show the phase boundary for the relaxed state proposed by McKernan *et al.* (Ref. 5). The dashed line is the phase boundary of the final FISDW phase for the relaxed state originally determined by Naughton *et al.* (Ref. 4). Solid and open circles indicate the FISDW transition temperature and the high-field phase boundary for our hydrogenated samples.

T. We confirm this behavior for our hydrogenated samples as shown in Fig. 5. On the other hand, T_{FISDW} in $d\text{-ClO}_4$ for $\mathfrak{R}_C = 0.0009$ K/s rapidly increases with increasing B up to 16 T and slightly decreases above 20 T as shown in Fig. 4. The different behavior of T_{FISDW} at high magnetic field between deuterated samples and hydrogenated ones is attributed to the difference of the chemical pressure in the crystal. It indicates that the negligible B dependence of T_{FISDW} above 15 T in hydrogenated samples is not intrinsic for slowly cooled $(\text{TMTSF})_2\text{ClO}_4$. In $d\text{-ClO}_4$ for 0.018 K/s, the B dependence of T_{FISDW} is almost the same as that for 0.0009 K/s. We observe, however, that β_{HI} (27 T) which is independent of temperature below 2.5 K decreases with increasing temperature above 2.5 K. Above 3.5 K, T_{FISDW} has been determined from the hump structure of R_0 which exists up to 4.2 K, although the sudden increase of R_0 becomes rounded. In $d\text{-ClO}_4$ for 0.67 K/s, β_{HI} is observed at about 23.5 T and T_{FISDW} increases with increasing B . The last semimetallic SDW phase between 9.7 T and β_{HI} is reduced from 5.5 to 4 K when the cooling rate \mathfrak{R}_C is increased. This result is consistent with the previous report¹³ for $h\text{-ClO}_4$, the interpretation of which will be discussed later. Thus the experimental results lead to the conclusions that, with increasing the cooling rate \mathfrak{R}_C , (i) the high field phase boundary β_{HI} shifts towards a lower field, (ii) the last semimetallic FISDW phase between 9.7 T and β_{HI} is suppressed, (iii) the FISDW insulating phase above β_{HI} in which the Hall voltage becomes almost zero⁵ is enhanced. These results mean that the last semimetallic FISDW phase and the FISDW insulating phase correspond to *different FISDW states*.

In order to explain this \mathfrak{R}_C dependence of the FISDW phase, we will now discuss the role of the dimerized gap due to anion ordering (AO) and that of the SDW nesting vector. As discussed in a previous report,¹³ the concentration of scattering centers associated with the boundaries between anion-ordered regions increases with increasing \mathfrak{R}_C . This is consistent with the fact that the residual resistance in the metallic phase increases with increasing \mathfrak{R}_C . For the slowly cooled ClO_4 salt, AO creates a superlattice potential [Fig. 6(b)] dividing the original Fermi surface into two pairs of open sheets. As a result, a dimerized gap due to AO is introduced in the electron band as shown in Fig. 6(a). Because the periodic anion potential is out of phase at the boundary between adjacent anion-ordered regions [Fig. 6(c)], for electrons moving across these boundaries, the dimerized gap due to AO is averaged out. These boundaries not only work as scattering centers but also suppress the dimerized gap due to AO. As a result, the effective dimerized gap due to AO decreases with increasing \mathfrak{R}_C . Perturbative calculations using the standard model have shown that in the case of a small superlattice potential V due to AO, the most stable SDW nesting vector Q_{SDW} is $(2k_F, \pi/b) = (2k_F, 0)$ [see Fig. 6(a)] and subphases with odd quantum numbers, i.e., $\dots, 5, 3, 1$, successively appear when the field is increased.^{15,16} Although this model can explain the phase diagram of slowly cooled $h\text{-ClO}_4$ below 8 T (Ref. 2) and the enhancement of the FISDW insulating phase above the high-field phase boundary β_{HI} with increasing \mathfrak{R}_C , the decrease of β_{HI} and the suppression of the last semimetallic SDW phase with in-

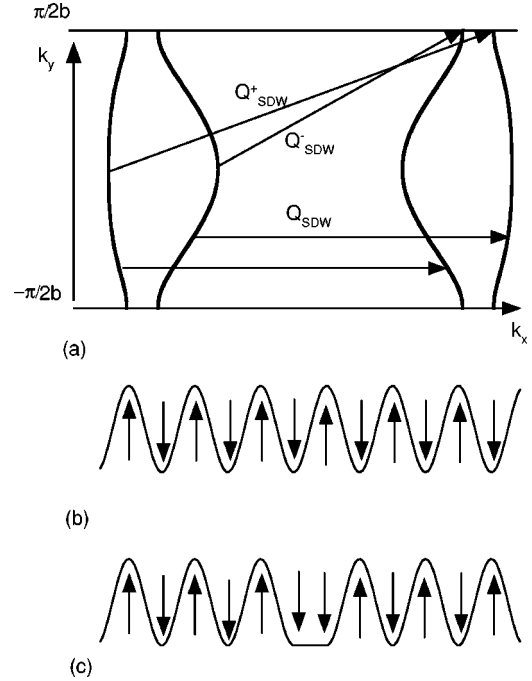


FIG. 6. (a) Schematic of the Fermi surfaces of $(\text{TMTSF})_2\text{ClO}_4$, resulting from a dimerization of the system along the b axis. $Q_{\text{SDW}} = (2k_F, \pi/b) = (2k_F, 0)$ and $Q_{\text{SDW}}^\pm = (2k_F^\pm, \pi/2b)$ are the SDW nesting vectors. (b) Periodic anion potential without the boundary between anion ordered states. (c) Anion potential with the boundary between anion ordered states.

creasing \mathfrak{R}_C cannot be explained within the standard model with small V .

On the other hand, McKernan *et al.* proposed the nesting of another pair of the two pairs of open orbit Fermi surface sheets separated by the superlattice potential.⁵ Using nonperturbative calculations Kishigi claimed that a new FISDW phase with a SDW nesting vector $Q_{\text{SDW}}^\pm = (2k_F^\pm, \pi/2b)$ as shown in Fig. 6(a) is stabilized for a large V .¹⁷ In fact, the magnitude of V estimated from the angular dependent magnetoresistance measurements is of the order of the interchain hopping integral t_b .¹⁸ Recent calculations for ClO_4 salt have pointed out that, when V is increased, the SDW state with Q_{SDW} is rapidly suppressed while the SDW state with Q_{SDW}^\pm becomes stable at higher value of V .^{19,20} Because the FISDW phase between 12 and 24 T is suppressed with increasing \mathfrak{R}_C , it is reasonable to estimate that the respective ground states of the last semimetallic FISDW phase and of the insulating FISDW phase are a $n=1$ state with Q_{SDW}^\pm and a $n=0$ insulating state with Q_{SDW} . Because the FISDW phase with Q_{SDW}^\pm becomes more stable with increasing the value of V , the model with Q_{SDW}^\pm can explain the decrease of β_{HI} and the suppression of the last semimetallic SDW phase. We are therefore led to conclude that β_{HI} of our experiment corresponds to the phase boundary between the Q_{SDW}^\pm phase and the Q_{SDW} phase. As shown in Fig. 5, the high-field phase boundary β_{HI} (a first-order transition) proposed by McKernan *et al.* is located at 3.5 K between 21 and 25 T.⁵ Their phase boundary is characterized by the step of Hall voltage and magnetization. They considered this phase boundary as

the FISDW transition of one pair of Fermi surface within the Q_{SDW}^{\pm} phase. As a result, the FISDW state at high magnetic fields can be separated three phases characterized by Hall voltage, magnetization, and the hump structure of R_0 . This FISDW phase diagram is consistent with that calculated by Kishigi.¹⁷ Accordingly, if we assume that the last semimetallic FISDW phase is the FISDW phase with Q_{SDW}^{\pm} stabilized by the dimerized gap due to AO, the \mathfrak{R}_C dependence of the FISDW transition and of β_{HI} in the hydrogenated and deuterated ClO_4 salts can be explained by the effective dimerized gap resulting from AO.

IV. CONCLUSION

We have measured the magnetoresistance, up to 28 T, in the SDW phase of hydrogenated and deuterated $(\text{TMTSF})_2\text{ClO}_4$, for various cooling rates \mathfrak{R}_C through the anion ordering temperature. We thus have obtained the \mathfrak{R}_C dependence of the FISDW transition temperature T_{FISDW} and of the phase boundary at high-magnetic fields. The deuteration of the ClO_4 salt works as a positive chemical pressure

in the crystal and moves the phase boundaries of FISDW towards the high-field side. The deuterated $(\text{TMTSF}-d_{12})_2\text{ClO}_4$ salt shows the FISDW phase in the wide cooling rate region which allowed us to investigate the \mathfrak{R}_C dependence of the FISDW phase in detail. We have found that, with increasing \mathfrak{R}_C , the high-field phase boundary β_{HI} is shifted towards a lower magnetic field, the last semimetallic SDW phase below β_{HI} is suppressed, and the FISDW insulating phase above β_{HI} is enhanced. The \mathfrak{R}_C dependence of T_{FISDW} and of β_{HI} can be explained by the mean-field theory by taking into account the FISDW phase with the SDW nesting vector Q_{SDW}^{\pm} stabilized by the dimerized gap due to anion ordering.

ACKNOWLEDGMENTS

The authors wish to acknowledge helpful discussions with Dr. K. Kishigi. Some of this work was carried out as part of the ‘‘Research for the Future’’ project, JSPS-RFTF97P00105, supported by the Japan Society for the Promotion of Science.

*Electronic address: mat@phys.sci.hokudai.ac.jp URL: <http://phys.sci.hokudai.ac.jp/LABS/nomura/english.html>

¹For a review, see T. Ishiguro, K. Yamaji, and G. Saito, *Organic Superconductors II* (Springer-Verlag, Berlin, 1998).

²M. Ribault, *Mol. Cryst. Liq. Cryst.* **119**, 91 (1985).

³R. V. Chamberlin, M. J. Naughton, X. Yan, L. Y. Chiang, S.-Y. Hsu, and P. M. Chaikin, *Phys. Rev. Lett.* **60**, 1189 (1988).

⁴M. J. Naughton, R. V. Chamberlin, X. Yan, S.-Y. Hsu, L. Y. Chiang, M. Ya. Azbel, and P. M. Chaikin, *Phys. Rev. Lett.* **61**, 621 (1988).

⁵S. K. McKernan, S. T. Hannahs, U. M. Scheven, G. M. Danner, and P. M. Chaikin, *Phys. Rev. Lett.* **75**, 1630 (1995).

⁶J. P. Pouget, G. Shirane, K. Bechgaard, and J. M. Fabre, *Phys. Rev. B* **27**, 5203 (1983).

⁷K. Sinzger, S. Hunig, M. Jopp, D. Bauer, W. Bietsch, J. U. von Schutz, H. C. Wolf, R. K. Kremer, T. Metzenthin, R. Bau, S. I. Khan, A. Lindbaum, C. L. Lengauer, and E. Tillmanns, *J. Am. Chem. Soc.* **115**, 7696 (1993).

⁸J. S. Brooks, R. G. Clark, R. H. McKenzie, R. Newbury, R. P. Starrett, A. V. Skougarevsky, M. Tokumoto, S. Takasaki, J. Yamada, H. Anzai, and S. Uji, *Phys. Rev. B* **53**, 14 406 (1996).

⁹F. Guo, K. Murata, H. Yoshino, S. Maki, S. Tanaka, J. Yamada, S. Nakatsuji, and H. Anzai, *J. Phys. Soc. Jpn.* **67**, 3000 (1998).

¹⁰W. Kang, S. T. Hannahs, and P. M. Chaikin, *Phys. Rev. Lett.* **70**, 3091 (1993).

¹¹H. Schwenk, E. Hess, K. Andres, F. Wudl, and E. Aharon-Shalon, *Phys. Lett.* **102A**, 57 (1984).

¹²Ok-Hee Chung, W. Kang, D. L. Kim, and C. H. Choi, *Phys. Rev. B* **61**, 11 649 (2000).

¹³N. Matsunaga, A. Briggs, A. Ishikawa, K. Nomura, T. Hanajiri, J. Yamada, S. Nakatsuji, and H. Anzai, *Phys. Rev. B* **62**, 8611 (2000).

¹⁴G. Montambaux, *Phys. Rev. B* **38**, 4788 (1988).

¹⁵A. G. Lebed and P. Bak, *Phys. Rev. B* **40**, 11 433 (1989).

¹⁶T. Osada, S. Kagoshima, and N. Miura, *Phys. Rev. Lett.* **69**, 1117 (1992).

¹⁷K. Kishigi, *J. Phys. Soc. Jpn.* **67**, 3825 (1998).

¹⁸H. Yoshino, A. Oda, T. Sasaki, T. Hanajiri, J. Yamada, S. Nakatsuji, H. Anzai, and K. Murata, *J. Phys. Soc. Jpn.* **68**, 3142 (1999).

¹⁹D. Zanchi and A. Bjielis, *Europhys. Lett.* **56**, 596 (2001).

²⁰K. Sengupta and N. Dupuis, *Phys. Rev. B* **65**, 035108 (2002).